DTU Library

Suspension-Firing of Biomass

Part 2, Boiler Measurements of Ash Deposit Shedding

Shafique Bashir, Muhammad; Jensen, Peter Arendt; Frandsen, Flemming; Wedel, Stig; Dam-Johansen, Kim; Wadenback, Johan

Link back to DTU Orbit

Suspension-Firing of Biomass. Part 2: Boiler Measurements of Ash Deposit Shedding

Muhammad Shafique Bashir,[†] Peter Arendt Jensen,*,[†] Flemming Frandsen,[†] Stig Wedel,[†] Kim Dam-Johansen,[†] and Johan Wadenbäck[‡]

[†]DTU Chemical and Biochemical Engineering, Building 229, Technical University of Denmark, DK-2800 Lyngby, Denmark
[‡]Vattenfall A/S, Amager Power Plant, Kraftværksvej 37, DK-2300 Copenhagen S, Denmark

ABSTRACT: This paper is the second of two papers, describing probe measurements of deposit buildup and removal (shedding), conducted in a 350 MW_{th} suspension-fired boiler, firing straw and wood. Investigations of deposit buildup and shedding have been made by use of an advanced online deposit probe and a sootblowing probe. The influences of feedstock (i.e., straw share in wood), flue gas temperature (600−1050 °C), probe surface temperature (500 and 600 °C), and probe exposure time on deposit shedding have been quantified. Quantification of naturally occurring deposit shedding and deposit shedding during plant sootblowing was made via deposit mass uptake signals obtained from the deposit probe. The deposit shedding process was characterized by calculation of the amount of deposit removed at a shedding event (g/m^2) and the frequency of the shedding events (h^{-1}). The results showed that the shedding process is stochastic and that the amount of deposit shed varies even at constant local conditions. However, the deposit shedding rates showed an increasing trend with increase in flue gas temperatures and probe deposit mass loads. The deposit shedding rate was in most cases higher at a probe temperature of 500 °C than at a probe temperature of 600 °C. A possible reason for this is partial melting and/or sintering of the innermost deposit layer (rich in K, Cl, and S) at higher probe surface temperature. This could cause the adhesion strength of the deposit to the probe to increase at the higher probe temperature. Quantification of the necessary peak impact pressure (PIP) needed to remove the deposit was also made by use of a sootblowing probe in conjunction with the deposit probe. Results of deposit removal by artificial sootblowing showed that the deposits formed on a 500 °C probe temperature and at exposure times of <91 h can be removed with a PIP of <55 kPa. However, increase in probe exposure time and/or probe surface temperature (600 °C) significantly increases the PIP needed to remove the deposits.

INTRODUCTION

The focus on substituting fossil resources by biomass has significantly increased the interest in efficient use of biomass for electricity production, and this includes the use of wood or straw in large suspension-fired boilers. However, especially straw constitutes a serious technical challenge with respect to deposit formation and corrosion, due to the large content of K and Cl in straw.[1−9] Deposit formation and corrosion problems limit the maximum applicable superheater temperature and, thereby, limit the electrical efficiency. In the case of severe ash deposition, boiler shutdown and expensive manual cleaning of the heat transfer surfaces may be needed. To minimize deposition problems, different strategies can be employed, for example, the use of additives that can convert gaseous inorganic species to less harmful forms, pretreatment of fuels by leaching out alkali, cofiring with coal, and the use of effective deposit-shedding techniques.[10−16] Use of additives and pretreatment of fuels by leaching are less cost-effective compared to the use of effective deposit shedding techniques.[7,10−14]

Ash deposit buildup during biomass combustion is a dynamic process consisting of both deposit formation[14,15] and shedding.[12,14,16] The most common industrial methods used to shed deposits from superheater tubes include sootblowing, mechanical vibrations, detonation wave techniques, shot-cleaning methods, thermal tensions, and rapping gear systems. Shedding may be initiated at the surface of the deposit, along the deposit tube interface, or inside the deposit depending on the local boiler conditions and the deposit properties. Important mechanisms of ash deposit shedding are[14,16] (1) erosion, when nonsticky, relatively large, and sharp-edged fly ash particles often rich in quartz collide with nonsticky areas on a deposit surface causing deformation (ductile deposits) and a cutting action (brittle deposits); (2) gravity shedding, when the gravity force exceeds the tube adhesion strength; (3) through temperature changes and differences in the thermal expansion coefficients of the tube and deposit; local temperature changes may be caused by sootblowing or boiler load fluctuations; and (4) mechanically induced tension in the deposit typically caused by vibrations or sootblowing.

These mechanisms include both naturally occurring and artificially induced shedding. Natural shedding includes processes such as surface melting, erosion, and thermal shock. Steam, water, and air sootblowing are the most common artificial shedding techniques applied to remove deposits from superheater tubes. Biomass-fired boilers often have several sootblowers depending on the local flue gas temperature, deposit-sintering characteristics, and deposit quantity.[14,16] The cleaning effectiveness depends on the sootblower location, the cleaning media applied, and the peak impact pressure (PIP) reached when sootblowing is performed.[16−19] Sootblowers

effectively remove fouling deposits, but to ensure maximum boiler thermal efficiency, cost-effective use of sootblowers is also important, because these may consume a significant percentage of the boiler steam production.[20] In addition, a high superheater temperature (>550 °C) is needed due to the corresponding increased electrical efficiency, and therefore deposit shedding at elevated superheater temperatures is of significant interest.[20] Optimization of plant sootblowing and other deposit shedding conditions is important to facilitate efficient removal of deposits from biomass-fired boilers.

Full-scale deposition and shedding measurements provide useful and real information with respect to better understanding of deposit shedding and minimizing fouling and slagging in biomass-fired boilers. Ash deposit shedding through surface melting in the high-temperature superheater region at the Avedøre straw grate-fired boiler was investigated by Zbogar et al.[21] The results showed that deposit surface melting is the main mechanism of straw ash deposit shedding, at flue gas temperatures >1000 °C. Deposit shedding in the Avedøre straw grate-fired boiler was investigated by Zhou et al.[20] by using an artificial sootblowing probe in the superheater region nearer the convective pass at flue gas temperatures between 700 and 800 °C. Most deposit shedding studies have been based on measurements in laboratory-scale equipment,[18,22] grate-fired boilers,[20,21] and Kraft recovery boilers,[23] whereas only a limited amount of data is available from biomass suspension-firing.[24−27]

The aim of this study was to investigate deposit buildup and shedding in a 350 MW_{th} suspension-fired boiler, firing straw and wood. Paper 1 in this series[24] dealt with deposit formation, whereas this paper deals with shedding. An advanced probe was used to collect ash deposits and shedding data, which are then used to quantify naturally occurring shedding and shedding caused by plant sootblowing.

■ EXPERIMENTAL SECTION

Boiler. The probe measurements were conducted at Amager Power Station, Unit 1 (AMV1). The AMV1 boiler is a multifuel suspension-fired boiler, which was commissioned in 2009 to fire pulverized biomass (in the shape of crushed pellets) with various shares of straw and wood. The annual biomass consumption (at AMV1) is approximately 300,000 tons of wood pellets and 100,000 tons of straw pellets. The 350 MW_{th} boiler is front wall-fired, having 12 burners located in three levels. Due to an expected increase in the corrosion rate with respect to temperature, the final steam temperatures of the superheaters are limited to approximately 540 °C.[28] The boiler data are shown in Table 1, whereas a schematic drawing of the boiler is shown in Figure 1 (more details can be seen in paper 1[24]).

Ash Deposition and Sootblowing Probe. The advanced deposit probe was made of stainless steel, about 3 m long with an outer diameter of 40.5 mm. More details of the deposit probe can be found in other publications.[21,24]

The flue gas temperature near the probe was continuously measured, using a simple thermocouple in a protective shell. In addition, a suction pyrometer (International Flame Research
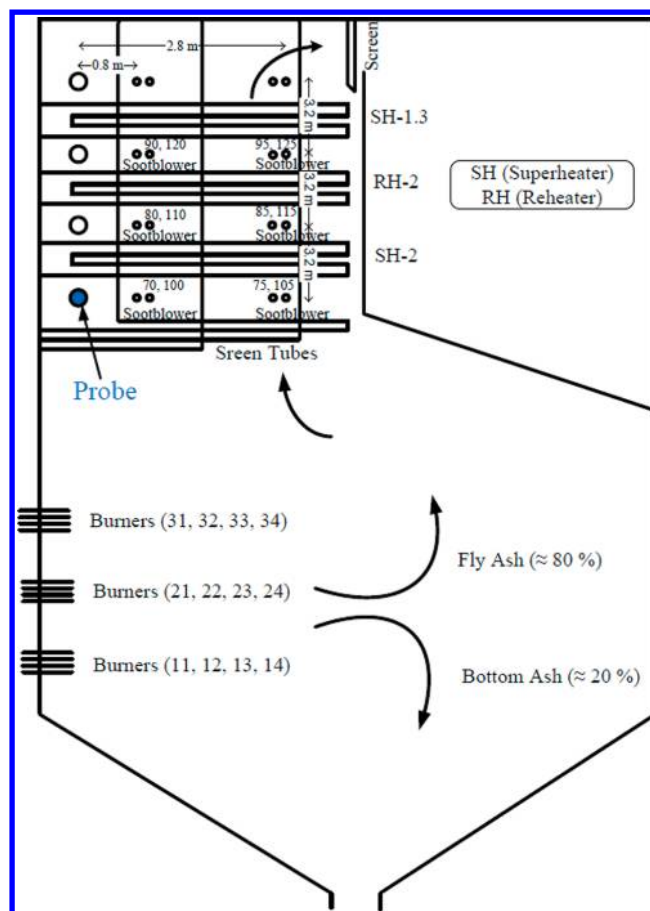

Figure 1. Schematic drawing of the AMV1 boiler outlining the position of the plant sootblowing near the experimental setup. In total, 12 sootblowers affect the deposit shedding process, 6 along the left wall of the boiler and 6 along the right wall of the boiler. The distance of each sootblower from the probe measuring position is also shown. Sootblower 70 was very near the probe measuring position (1 m to the left) and was shut down during tests 1−5. The first number in a pair of two numbers shows the sootblowers located on the same wall where the probe is located (left wall, burner location), whereas the second number shows the sootblowers located on the opposite wall (right wall, burner location).

Foundation model, IFRF[29]) was also used for shorter periods in each test, to find the difference between the thermocouple flue gas temperature measurements and the true flue gas temperature measurements. On the basis of these data, corrected thermocouple temperatures were calculated (see paper 1[24]). A charge-coupled device (CCD) camera was used to register the deposit formation and shedding processes on the probe. A schematic of the complete port setup used during the measurements can be seen in paper 1.[24]

An artificial sootblowing probe with an external diameter of 42.2 mm and a length of 3 m was used for in situ removal of deposits. The schematic drawing of the sootblowing probe is shown in Figure 2a, and the detailed sootblower nozzle drawing can be seen in Figure 2b. The air pressure to the sootblowing probe was measured by using a pressure gauge, and the air pressure was increased in steps. The sootblowing probe was cooled by water. In the large port (please refer to part 1 of the current series of paper[24]), a small port for the ash deposition probe, a port for the thermoelement, a CCD camera port, and a port for artificial sootblowing probe were placed. The sootblowing probe was placed parallel to the deposit probe. The sootblower probe nozzle was of convergent−divergent shape, and air at a supply pressure of 6.0 bar was fully expanded.[17] The sootblower nozzle was fixed at the end of the probe. The PIP of the nozzle was measured along the axial centerline as a function of the supplied air

Table 1. Brief Operational Data of the AMV1 Boiler

boiler cross-sectional area (at probe measuring position)	5.75 × 12.5 ~12 m²	
parameter (steam)	high-pressure (HP) superheater	reheater (RH)
temperature (°C)	540 (biomass)	540
pressure (bar)	185	75
flow (kg/s)	138.4	123
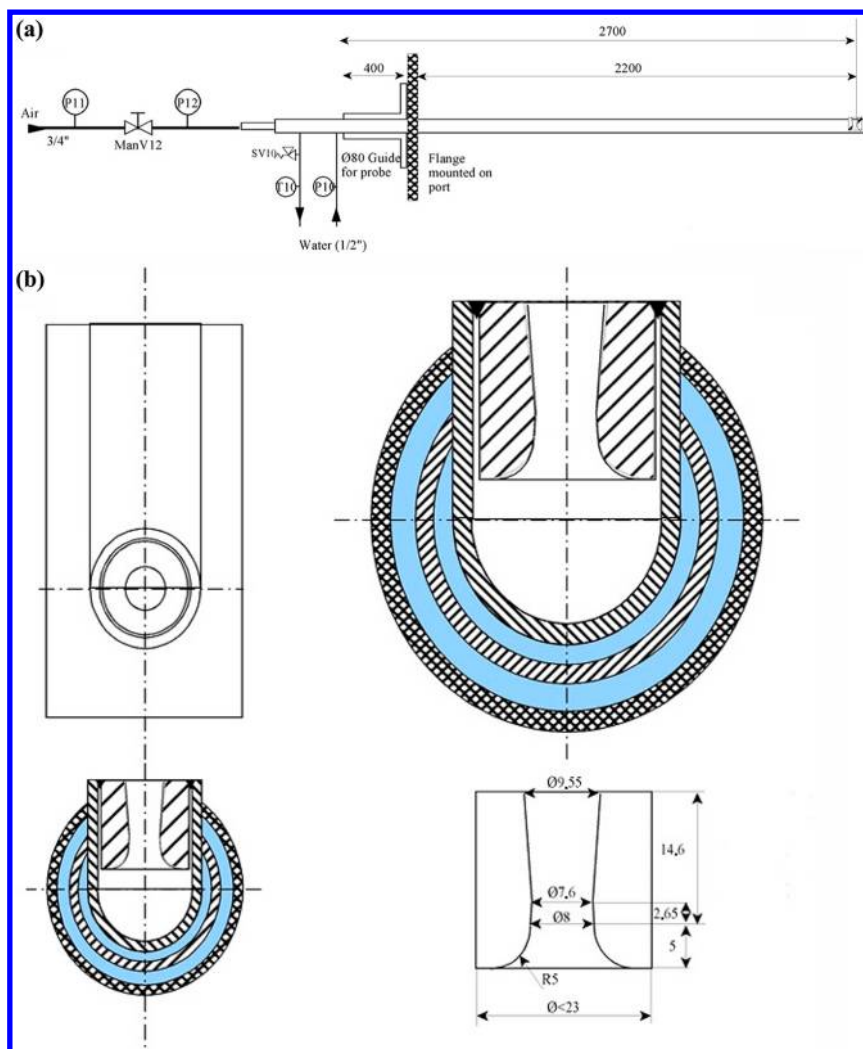
Figure 2. (a) Schematic of sootblowing probe with water and air flow description: P10, P11, and P12 are pressure gauges for air, P10 is a pressure gauge for water (to act as a cooling medium), and T10 is temperature indicator. (b) Detailed drawings of the sootblowing nozzle.

pressure in the laboratory at room temperature. The PIP of the jet, defined as the centerline stagnation pressure of the jet, was used to define the removal of deposits by the sootblowing probe.[17] The measured values of PIP are shown in Figure 3, and it is important to note that these values are measured at room temperature. In the applied range of PIP, there can be a minor impact of flue gas temperature on PIP, but the measurement of PIP at temperatures close to the flue gas temperature was not possible. The measured PIP increases with the supplied air pressure and drops off quickly with the axial distance from the nozzle exit (Figure 3).

Fuels. During the measurements, fuels were continuously sampled before the burners. The total ash contents of the fuel samples collected from all test runs were analyzed, and thereby the straw fuel fractions were determined on the basis of the total ash contents. In some cases also detailed ash analysis was made as shown in Table 2. The analysis methods and the detailed ash analysis of pure fuels and some samples from tests 1 and 5 are shown in Table 2. It is seen that the straw ash has high contents of Si, K, Cl, and Ca.

Overall, eight test runs were carried out, and the mean straw share during each test is shown in Table 3. The slight difference in fuel ash contents shown in Tables 2 and 3 is due to the fact that in Table 3 mean values of each complete test are shown, whereas in Table 2, values are shown for a sample collected just before the burners. It is also important to mention that pure straw and wood fuel samples shown in Table 2 were collected from the fuel silos, whereas fuel sample just before the burners was collected almost each day during each test. In the start of test 5, the fraction of straw in fuel was low

(about 14 wt %, not shown in Table 2); therefore, the overall percentage of straw in fuel was low compared to the fuel samples of test 5 shown in Table 2.

Procedure of Experiments. *Ash Deposition Experiments.* Measurements were conducted in the superheater region, just above the screen tubes (Figure 1). The influence of fuel type (straw share in wood), flue gas temperature (600−1050 °C), probe surface temperature (500 and 600 °C), and deposit mass load on ash deposit formation rate was investigated. Description of ash deposition equipment and detailed interpretation of results can be found in paper 1.[24]

Evaluation of probe heat uptake as a function of deposit mass load was also made for each test. A complete overview of all the conducted measurements is presented in Table 3. Additional information, for example, air flow rate, fuel flow rate, ash flux, etc., of each test is also shown in Table 3.

Artificial Sootblowing Experiments. Three different methods were used to quantify the PIP needed to remove the deposits on the probe (see Figure 4). In method 1, the sootblowing probe was placed parallel to the ash deposition probe and artificial sootblowing was started from the tip of the deposition probe with air pressure ranging from 0.5 to 4.0 bar. Method 2 is actually a continuation of method 1, where the sootblowing probe was slightly pulled out (approximately 20 cm) to remove remaining layers of the deposits by using the same principle adopted in method 1. This procedure was repeated until the nozzle of the sootblowing probe reached a distance of 1.5 m from the tip of the ash deposition probe. If the amount of deposits removed was not
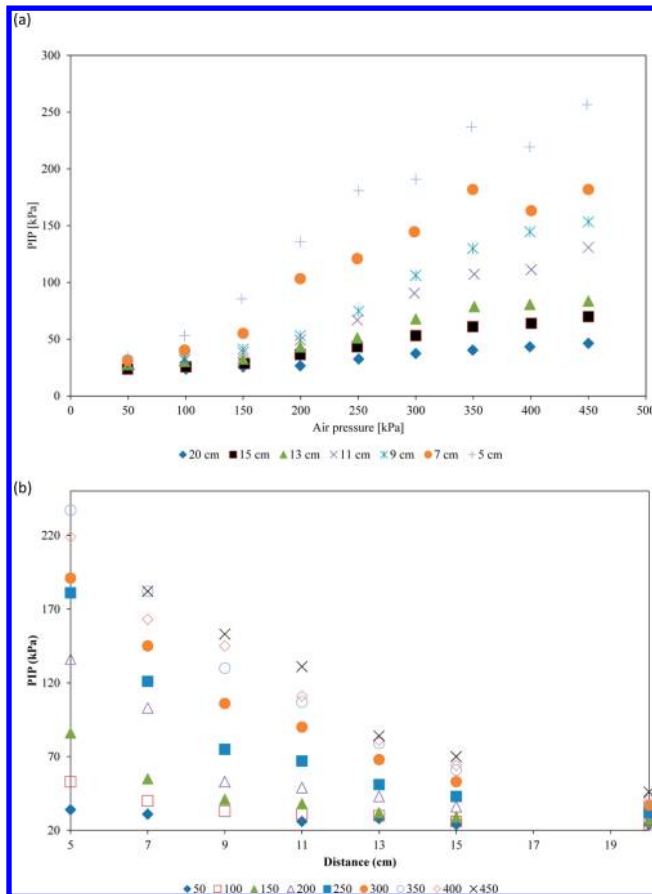
Figure 3. Measured peak impact pressure (PIP) as a function of (a) applied air pressure at various downstream distances from the nozzle exit to the deposit probe at room temperature and (b) distance from the nozzle exit to the deposit probe at various pressures at room temperature.

significant, method 3 was applied by reducing the distance between the nozzle and the deposition probe in the range of 5−20 cm, to achieve maximum values of PIP. In each position, the impact of air on the deposit probe was from a couple of seconds to a minute. In addition, in each method, the air pressure was increased in steps. The sootblowing probe was not rotated and was only pulled or moved closer to the deposit probe. During the artificial sootblowing, camera images were collected to confirm the observed changes in the deposit mass uptake signals.

Plant Sootblowing. In the superheater region area of the boiler, retractable steam sootblowers were used for a time of 5−10 min (each sootblower) at regular intervals during boiler operation, typically at 8 h intervals. Six sootblowers were placed along the left wall of the boiler and six along the right wall of the boiler as shown in Figure 1. The sootblower located nearest the probe measuring position (approximately 1 m to the left) was shut down during tests 1−5, whereas the rest of the sootblowers located farther away from the probe measuring position were in operation during all tests.

■ RESULTS AND DISCUSSION

Ash Deposit Formation Rate. The total amount of deposit collected on the probe is a function of both the deposit formation process and shedding events. Two different measures of deposit formation rate were used in the analysis of the data. The first is the integral deposit formation rate (IDF rate) found by dividing the integral mass change over integral time intervals (on the order of several hours) by the time interval. A second measure, the derivative-based deposit formation rate (DDF

rate), was determined by averaging the deposit mass uptake signals over short time intervals (on the order of minutes), calculating the local values of the time derivative of the mass uptake, removing large negative values signifying major shedding events, and finally time smoothing the derivatives to remove excessive noise. Further details about the deposit formation rate determinations are presented in paper 1.[24]

Video Observations of Shedding Events. The deposit mass uptake signals were continuously monitored, and deposit-shedding events were confirmed by video recordings. The deposit mass uptake signals during test 1 are shown in Figure 5. We have divided the shedding events into naturally occurring events and sootblowing-initiated shedding events. Even when the nearby sootblower is turned off, the increased thermal and mechanical fluctuations induced by the rest of the sootblowers may increase the shedding rate. No artificial probe sootblowing measurements were conducted during test 1.

Confirmation of some deposit shedding events was made using the images collected at 20−30 s intervals. It was found that deposit shedding was primarily through debonding from the surface of the deposit probe; an example of a deposit shedding event is shown in Figure 6. No deposit shedding through surface melting was seen in the videos collected from any of the tests, even though a flue gas temperature of >1000 °C was observed during tests 4 and 5. Earlier investigations by Zbogar et al.[21] showed shedding through surface melting in a straw grate-fired boiler, at local flue gas temperatures >1000 °C. Possibly the high contents of Si and Ca in the fly ash of the AMV1 boiler, and the relatively lower concentrations of the inorganic volatile elements (K, Cl, and S), cause a higher melting temperature of the ash deposits generated by the suspension-cofiring of straw and wood.[24,30]

Monitoring of deposit shedding from inspection holes very close to the port position revealed a small amount of deposit shedding through erosion when nonsticky, relatively large, and sharp-edged SiO_2-rich fly ash particles collide with nonsticky areas on a deposit surface. A significant amount of Si in the fly ash formed during straw and wood suspension-firing has been reported.[24,30] Generally, most of the deposits were removed by debonding, where larger pieces detached from the tube surface.

Deposit Removal (Shedding). As discussed in paper 1,[24] during the calculation of DDF rates, a particular negative slope cutoff level was selected to determine major shedding events accurately while still giving a satisfactory prediction of apparent DDF rates. The selected cutoff level was −3800 g/m²/h for all tests.[24] This cutoff level strikes a balance between including larger shedding events in the analysis and preventing deposit mass signal noise from being counted on a shedding event.[24] The selected minimum magnitude of a shedding event included in the analysis was −105 g/m², and this was calculated by eq 1.

minimum shedding event magnitude

$$= \text{slope cutoff level} \times \text{sampling interval}$$

$$= -3800 \frac{\text{g}}{(\text{m}^2\text{h})} \frac{\text{h}}{(3600\text{s})} \times 100\text{s}$$

$$= -105 \frac{\text{g}}{\text{m}^2} \tag{1}$$

The flue gas temperature and deposit probe mass uptake signals are shown in Figure 5 for test 1. The temperature measurements by the thermocouple show temperature fluctuations in the range of 500−800 °C. The deposit mass

Table 2. Analysis of Straw and Wood Pellets Used at AMV1[a]

parmeter	procedure	straw, Køge	wood, Kunda[b]	80−85% straw, test 1	65−70% straw, test 5	60−65% straw, test 5	60−65% straw, test 5	40−45% straw, test 5
date				March 22, 2010	April 19, 2010	April 20, 2010 (1:00 p.m.)	April 20, 2010 (5:00 p.m.)	April 21, 2010
ash contents (wt %, ar)	EN 14775:2009	6.03	0.80	5.26	4.32	3.56	3.63	2.74
ash contents (wt %, db)	EN 14775:2009	6.54	0.86	5.63	4.57	3.78	3.84	2.88
moisture (wt %, ar)	EN 14774-3:2009	7.86	6.83	6.67	5.61	5.94	5.55	5.03
higher heating value (MJ/kg, db)	EN 14918:2010	18.71	20.47	17.62	19.68	19.39	19.35	19.87
volatiles (wt %, db)	EN 15148:2009	80.91	85.24	82.87	82.58	82.15		83.11
C (wt %, db)	CEN/TS 15104:2006	50.52	55.54	51.16	52.44	52.89	52.57	53.91
S (wt %, db)	CEN/TS 15289:2006	0.15	0.035	0.121	0.105	0.095	0.093	0.068
N (wt %, db)	DS/EN ISO 10304-1:2009	0.59	0.73	0.8	0.62	0.63	0.68	0.75
H (wt %, db)	EN 14918:2010 calculated	5.79	6.15	5.85	5.92	5.97	5.96	6.02
O (wt %, db)	EN 14918:2010 calculated	36.11	36.68	36.43	36.19	36.45	36.67	36.28
Cl (wt %, db)	DS/EN ISO 10304-1:2009	0.290	0.003		0.155	0.184	0.191	0.093
ash analysis (wt %, db)								
Al_2O_3	DIN 51729/ASTM3682	0.66		0.95	1.88	1.30	0.97	2.11
CaO	DIN 51729/ASTM3682	14.56		8.30	9.97	11.05	11.80	17.69
Fe_2O_3	DIN 51729/ASTM3682	0.50		0.47	6.81	1.03	0.58	1.13
K_2O	DIN 51729/ASTM3682	17.88		15.25	12.58	15.92	20.41	13.96
MgO	DIN 51729/ASTM3682	3.39		2.25	2.11	2.29	2.54	2.90
Na_2O	DIN 51729/ASTM3682	0.69		0.57	0.59	0.87	1.04	1.03
P_2O_5	DIN 51729/ASTM3682	5.56		2.47	2.17	2.46	2.60	2.13
SO_3	DIN 51729/ASTM3682	2.43		2.36	2.03	2.16	1.88	2.43
SiO_2	DIN 51729/ASTM3682	44.51		52.05	44.89	49.15	46.95	36.87
TiO_2	DIN 51729/ASTM3682	0.05		0.06	0.11	0.10	0.06	0.13

[a]ar, as received; db, dry basis. [b]One type of four.

Table 3. Experimental Summary

	test 1	test 2	test 3	test 4	test 5	test 6	test 7	test 8
date	March 22−25, 2010	March 27−29, 2010	March 29−April 6, 2010	April 6−9, 2010	April 15−22, 2010	May 7−25, 2010	May 25−June 8, 2010	June 8−18, 2010
straw (wt %)	80−85	60−65	30−35	40−50	40−50	0−10	0−10	0−10
fuel ash content (wt %)	~5.2	~4.0	~2.4	~3.4	~3.4	~1.0	~1.0	~1.0
fuel flow (kg/s)	12.1	11.4	12.9	17.3	12.7	14	12	12
air flow (kg/s)	114	103	106	130	107	124	116	112
ash flux (approx) (g/m²/h)	25334	19382	12780	23741	17105	4439	4826	4272
probe temperature (°C)	500	600	500	500	500 (600)	550	550	550 (600)
exposure time (h)	56	45	185	73	168	434	335	212
probe heat uptake investigation	yes	yes	yes	yes	yes	yes	yes	yes
artificial sootblowing	no	yes	yes	yes	yes			
naturally occurring deposit shedding events	yes	yes	yes	yes	yes			
plant sootblowing	yes[a]	yes[a]	yes[a]	yes[a]	yes[a]	yes	yes	yes

[a]Plant sootblower very near the ash deposition probe (about 1 m to the left) was closed.

uptake signals show both natural and plant sootblowing shedding events. The deposit mass uptake signal is influenced by several processes: large shedding events, smaller shedding events (observed as a sudden deposit mass loss on the curve), a relatively slow deposit buildup process, and some noise mainly caused by boiler fluctuations. Boiler fluctuations could be mechanical vibrations or large changes in boiler flow dynamics. The most severe fluctuations are observed when the boiler plant sootblowers were used. Even though the plant sootblower very near the probe was shut down, the rest of the sootblowers to some extent induced fluctuations that could cause some shedding. All shedding events are marked showing both natural
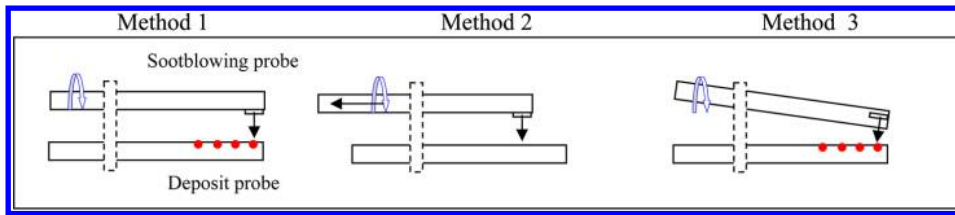
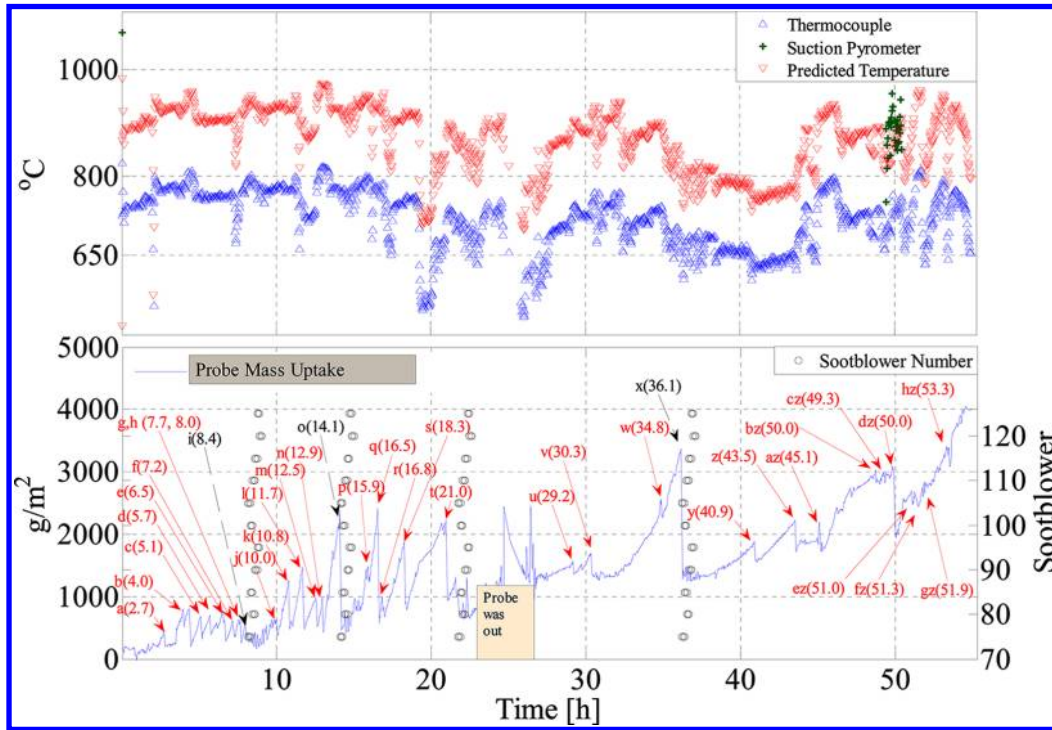**Figure 4.** Experimental methods applied for artificial sootblowing.

Figure 5. Data of flue gas temperature (thermocouple, suction pyrometer, and predicted[24]), probe mass uptake, and plant sootblowing events (specific number of sootblower in operation as seen on the secondary *y*-axis) during test 1 with identified shedding events. Red arrows with continuous line show natural deposit shedding events, whereas black arrows with discontinuous line show deposit shedding through plant sootblowing. Sootblower number shown on the secondary *y*-axis represents a specific sootblower in the superheater region shown in Figure 1. The number attached to each event specifies the time of the shedding event.
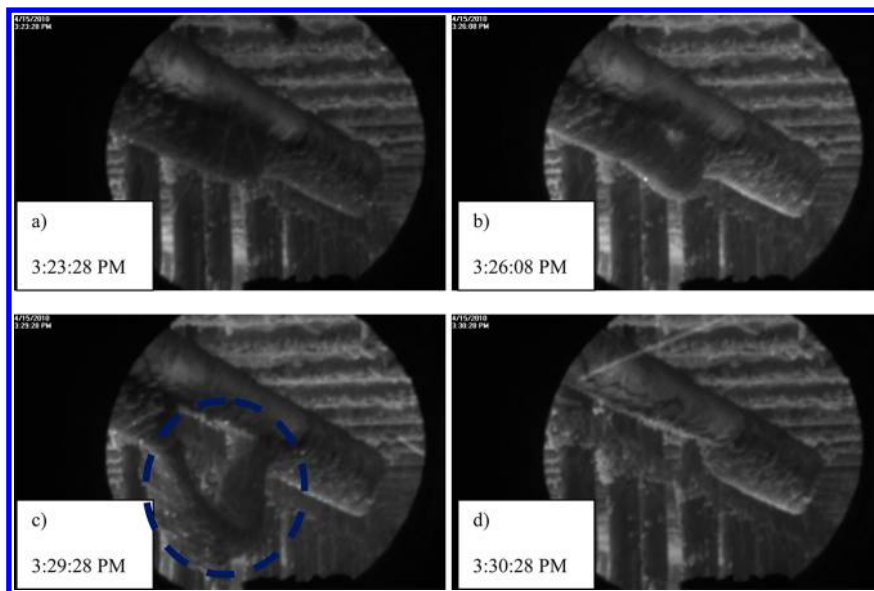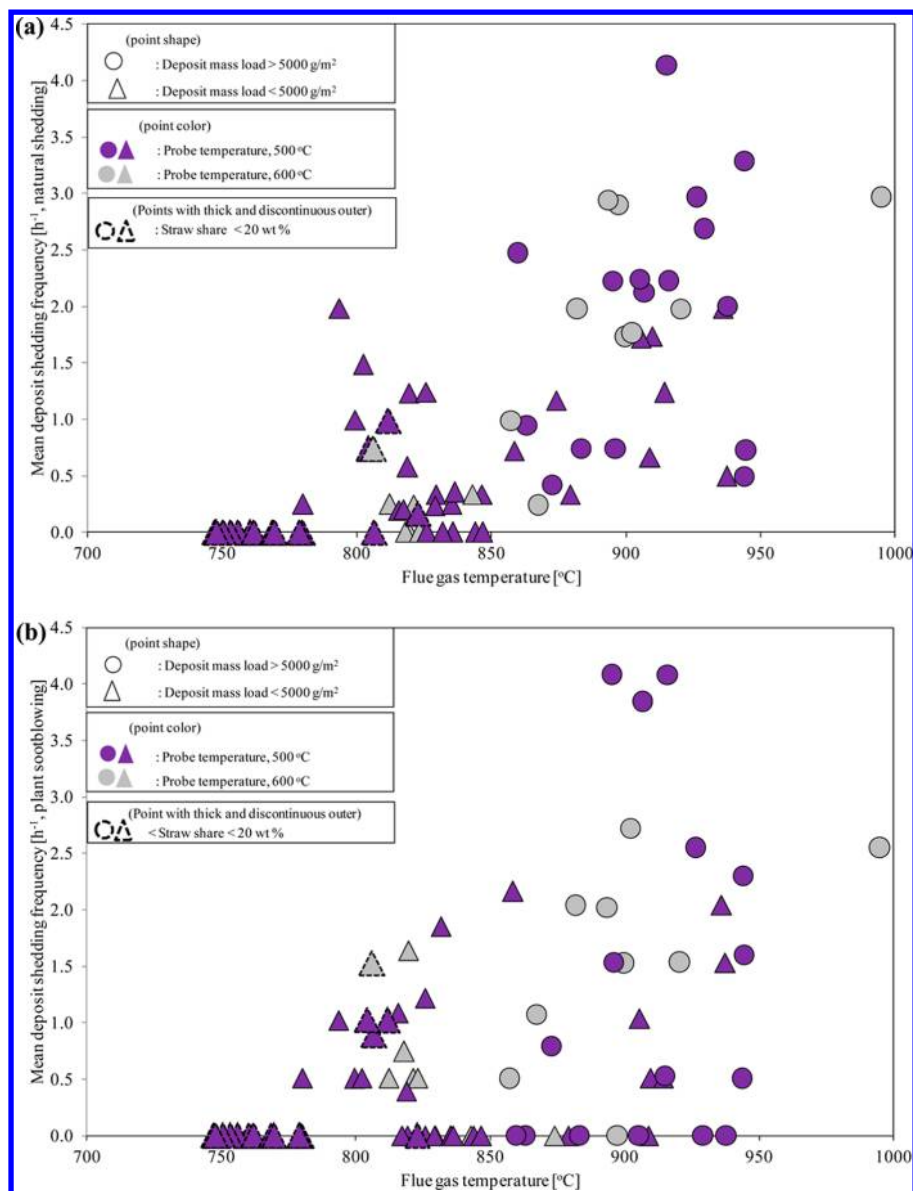

Figure 6. Images of the ash deposition probe during test 5 on May 15, 2010 (about 4 h of exposure time). From panels a to d, the process of natural deposit shedding through debonding can be clearly seen.

Figure 7. Impact of flue gas temperature on (a) mean natural deposit shedding frequency and (b) mean plant sootblowing shedding frequency. Data points are from tests 1−5. The particular point shape represents the deposit mass load, and the color represents the probe surface temperature, whereas points (larger in size) with thick and discontinuous outer edges are representative of straw share in wood.

and plant sootblowing-induced shedding events. The naturally occurring shedding was defined to occur when the plant sootblowers were not in operation, and no artificial sootblowing tests were made. Sootblowing-induced shedding events can occur when the plant sootblowers are in operation. Typically, a plant sootblowing operation lasts for about 1−2 h. The lengths of intervals between naturally occurring shedding incidents are very variable as seen in Figure 5. In the first 10−12 h, natural shedding occurs often, but with only small amounts of material. From about 12 to 21 h, the intervals between shedding events become longer, and the amounts removed in the single events are also larger compared to the previous period. Finally, from 29 to 55 h, natural shedding is infrequent, but the shedding amount is again relatively small. These changes in behavior may be related to varying boiler operation parameters, but it is worth noting that during the full 55 h, the baseline of deposited mass on the probe increased slowly from 0 to about 2500 g/m². Similar behavior was observed in most of the other tests also.

Under these conditions, analysis and quantification of natural shedding during the long time test is done by averaging over shorter time intervals. These are long enough that short time random behavior does not influence results unduly, but short enough that local operating and probe conditions may be considered fairly constant. Thus, each test was divided into sections of 6 h, which were used for the data analysis to characterize the deposit shedding by means of magnitude of events (g/m²) and the incidence rate (deposit shedding frequency, h⁻¹). With regard to natural shedding, this allowed us to calculate mean incidence rates (mean natural deposit shedding frequency), $f_{nat,6}$, as the number of shedding events in a 6 h interval divided by the interval time. It should be noted that for each 6 h interval, the period of plant sootblowing was excluded in the evaluation of the natural shedding events. The mean deposit shedding frequency by natural shedding was calculated by eq 2.
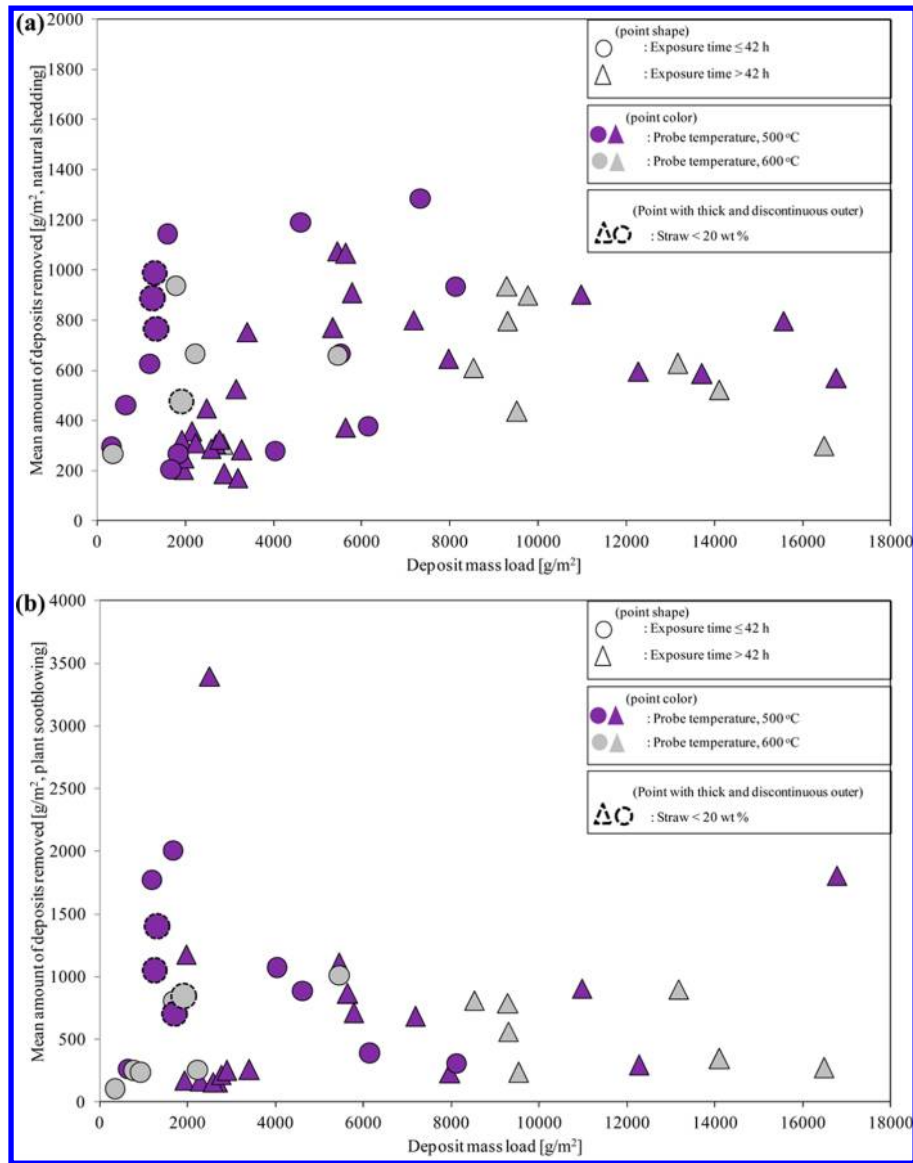
Figure 8. Impact of deposit mass load on (a) the mean amount of deposits removed naturally and (b) the mean amount of deposits removed by plant sootblowing. Data points are from tests 1−5. The particular point shape represents the exposure time, and the color represents the probe surface temperature, whereas points (larger in size) with thick and discontinuous edges are representative of straw share in wood.

mean natural deposit shedding frequency $(f_{nat,6})$

$$= \frac{\text{no. of natural shedding events in a 6 h interval}}{\text{total time without plant sootblowing during a 6 h interval}} \quad (2)$$

The mean plant sootblowing deposit shedding frequency was calculated by eq 3,

mean plant sootblowing deposit shedding frequency $(f_{soot,6})$

$$= \frac{\text{no. of plant sootblowing shedding events in a 6 h interval}}{\text{total time of plant sootblowing during a 6 h interval}} \quad (3)$$

Influence of Different Parameters on the Shedding Process. The shedding frequency (h^{-1}) and the shedding event size (g/m^2) are shown in Figures 7 and 8. The mean values for 6 h periods with similar conditions are presented in Tables 4 (natural shedding) and 5 (sootblowing induced shedding). The shedding data are divided into groups to make it possible to analyze the influence of changed conditions in flue gas temperature (above or below 850 °C), probe surface

temperature (500 or 600 °C), straw fuel share (weight fraction of straw in the fuel above or below 20%), and deposit mass load (above or below 5000 g/m^2). The selected criterion of flue gas temperature is based on the results presented in paper 1,[24] where it was found that the deposit formation rate increases significantly when the flue gas temperature exceeds 850 °C. The second criterion was the probe surface temperature to investigate the influence of probe surface temperature on deposit shedding. The selected number (5000 g/m^2) for the deposit mass load is an arbitrary number, which was introduced to find any impact of deposit amount on the probe on deposit shedding. As seen in Tables 4 and 5 several of the combinations of operating conditions are without data. In two cases (straw < 20 wt %, deposit mass load < 5000 g/m^2, flue gas temperature < 850 °C, probe surface temperature = 600 °C; and straw > 20 wt %, deposit mass load < 5000 g/m^2, flue gas temperature >850 °C, probe surface temperature = 600 °C) only one 6 h period is presented. These cases are highlighted in italic type in Tables 4 and 5, and statistically it is difficult to use those data because of

Table 4. Summary of the Analysis of Natural Deposit Shedding for Two Different Sets of Flue Gas Temperature, Probe Surface Temperature, Straw Share, and Deposit Load

natural deposit shedding		flue gas temperature:	<850 °C		>850 °C	
fuel straw share	probe deposit mass load	probe surface temperature:	500 °C	600 °C	500 °C	600 °C
>20 wt %	>5000 g/m^2	mean DDF rate (g/m^2/h)			2691	1934
		no. of 6 h periods			16	9
		no. of shedding events			134	70
		mean size of shedding event (g/m^2)			854	730
		mean deposits removed (%)			10	7
		mean shedding frequency (h^{-1})			1.89	1.92
		mean shedding rate (g/m^2/h)			1612	1403
	<5000 g/m^2	mean DDF rate (g/m^2/h)	234	313	1245	577
		no. of 6 h periods	19	6	8	1
		no. of shedding events	42	4	38	7
		mean size of shedding event (g/m^2)	343	702	632	305
		mean deposits removed (%)	15	34	27	10
		mean shedding frequency (h^{-1})	0.47	0.15	1.04	1.17
		mean shedding rate (g/m^2/h)	160	107	660	356
<20 wt %	>5000 g/m^2	mean DDF rate (g/m^2/h)				
		no. of 6 h periods				
		no. of shedding events				
		mean size of shedding event (g/m^2)				
		mean deposits removed (%)				
		mean shedding frequency (h^{-1})				
		mean shedding rate (g/m^2/h)				
	<5000 g/m^2	mean DDF rate (g/m^2/h)	221	1913		
		no. of 6 h periods	17	1		
		no. of shedding events	8	3		
		mean size of shedding event (g/m^2)	910	476		
		mean deposits removed (%)	44	28		
		mean shedding frequency (h^{-1})	0.11	0.74		
		mean shedding rate (g/m^2/h)	101	353		

the limited data points. Below the influence of local changes and changes in probe conditions on the shedding characteristics is discussed.

(a) Increased Deposit Load on the Probe. The mean amount of deposit removed at a shedding event is 716 g/m^2 during natural shedding and 805 g/m^2 during sootblowing-initiated shedding as seen in Figure 8. There are seen large fluctuations in the amount of deposit removed in a single shedding event (6 h mean) from 180 to 1400 g/m^2 during natural shedding, but there is not observed any strong influence of the total deposit mass load on the amount of deposit removed in the single event (see Figure 8). In most cases, the probe deposit mass increases over time, and in the later stages of the experiments more than 5000 g/m^2 deposits are collected on the probe.

Two sets of data with similar conditions except for an increase in deposit load are available only for a flue gas temperature >850 °C, a probe temperature of 500 °C, and a straw fuel share >20 wt % (as seen in Tables 4 and 5). Going from a deposit mass below 5000 g/m^2 to above 5000 g/m^2 changed the mean shedding event mass from 632 to 854 g/m^2 during natural shedding and from 935 to 849 g/m^2 during sootblowing-induced shedding. Again, this shows that even though the deposit mass level has a tendency to increase through time, this does not strongly influence the amount of deposit released at a shedding event. The shedding frequency is increased from 1.04 to 1.89 h^{-1} during natural shedding and from 1.29 to 1.56 h^{-1} during sootblower-induced shedding for the change from a deposit mass below 5000 g/m^2 to above

5000 g/m^2. There is also seen a clear increase in DDF rate when the deposit mass load is increased, and because the shedding frequency increases, the shedding rate (g removed/h/m^2) increases with the increasing deposit mass load.

Because the amount of deposit removed at a shedding event is approximately independent of the amount of deposits on the probe, the relative amount of deposits removed (relative to total amount on the probe) is larger at low probe deposit mass. In addition, video recordings of deposit removal by plant sootblowing indicate that for shorter probe exposure time, plant sootblowing removes deposits from the entire surface of the probe, whereas a complete or partial layer of deposits is removed at higher exposure times.

With regard to the shedding properties, an increased amount of deposits on the probe leads not to a significant change in the amount of deposit lost at a shedding event but to an increase in the shedding frequency and thereby the shedding rate.

(b) Changed Probe Surface Temperature. For two sets of data (temperature < 850 °C, deposit mass < 5000 g/m^2, and a straw fuel share > 20 wt %; and temperature > 850 °C, deposit mass > 5000 g/m^2, and a straw fuel share > 20 wt %) in Tables 4 and 5, the influence of a change in probe temperature from 500 to 600 °C is illustrated. However, no clear tendencies are observed, and a systematic change in the amount of deposit shed in an event or the deposit frequency cannot be observed when the probe temperature is changed from 500 to 600 °C. However, if one looks at the mean shedding rate, then the shedding rate is in most cases higher at a probe temperature of

Table 5. Summary of the Analysis of Shedding during Sootblower Operation for Two Different Sets of Flue Gas Temperatures, Probe Surface Temperatures, Straw Shares, and Deposit Loads

sootblowing deposit shedding		flue gas temperature:	<850 °C		>850 °C	
fuel straw share	probe deposit mass load	probe surface temperature:	500 °C	600 °C	500 °C	600 °C
>20 wt %	>5000 g/m²	mean DDF rate (g/m²/h)			2691	1934
		no. of 6 h periods			16	9
		no. of shedding events			39	30
		mean size of shedding event (g/m²)			849	688
		mean deposits removed (%)			10	9
		mean shedding frequency (h⁻¹)			1.56	1.71
		mean shedding rate (g/m²/h)			1322	1176
	<5000 g/m²	mean DDF rate (g/m²/h)	234	313	1245	
		no. of 6 h periods	19	6	8	
		no. of shedding events	9	5	15	
		mean size of shedding event (g/m²)	750	332	935	
		mean deposits removed (%)	20	32	42	
		mean shedding frequency (h⁻¹)	0.37	0.51	1.29	
		mean shedding rate (g/m²/h)	278	170	1208	
<20 wt %	>5000 g/m²	mean DDF rate (g/m²/h)				
		no. of 6 h periods				
		no. of shedding events				
		mean size of shedding event (g/m²)				
		mean deposits removed (%)				
		mean shedding frequency (h⁻¹)				
		mean shedding rate (g/m²/h)				
	<5000 g/m²	mean DDF rate (g/m²/h)	221	1913		
		no. of 6 h periods	17	1		
		no. of shedding events	8	3		
		mean size of shedding event (g/m²)	965	845		
		mean deposits removed (%)	69	46		
		mean shedding frequency (h⁻¹)	0.27	1.53		
		mean shedding rate (g/m²/h)	260	1293		
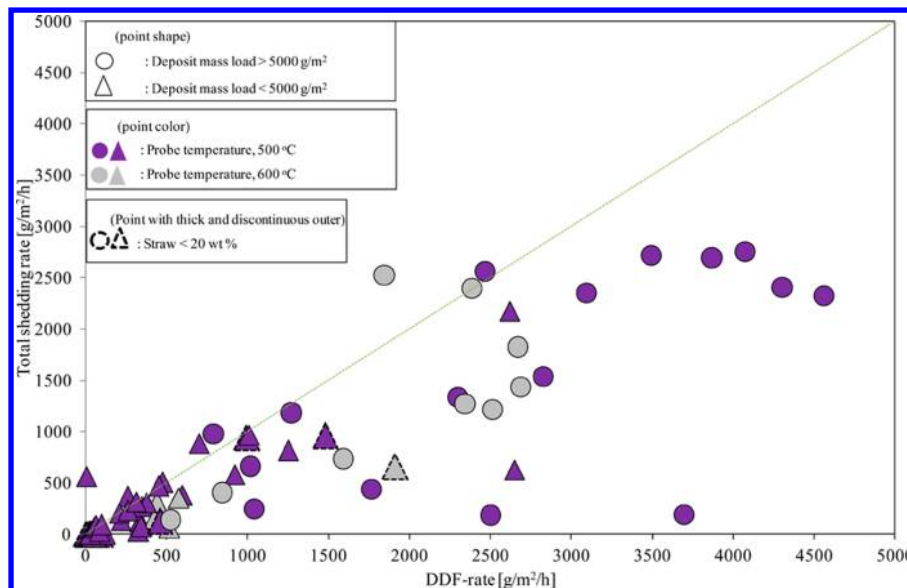
Figure 9. Total deposit shedding rate as a function of the DDF rate. Data points are from tests 1−5. The particular point shape represents the deposit mass load, and the color represents the probe surface temperature, whereas points (larger in size) with thick and discontinuous edges are representative of straw share in wood.

500 °C than at a probe temperature of 600 °C, possibly due to partial melting and/or sintering of the innermost deposit layer (rich in K, Cl, and S)[24] at higher probe surface temperature.

(c) Changed Flue Gas Temperature. As seen in Figure 7 an increased flue gas temperature leads to an increased deposit shedding frequency; even there is seen a very large spread in the data points. By comparison of the data sets with similar

Table 6. Mean DDF Rates and Mean Net Deposit Accumulation Rates for Two Different Sets of Flue Gas Temperatures, Probe Surface Temperatures, Straw Shares, and Deposit Loads

fuel straw share	probe deposit mass load	flue gas temperature:	<850 °C		>850 °C	
		probe surface temperature:	500 °C	600 °C	500 °C	600 °C
>20 wt %	>5000 g/m² (9403)ᵃ	mean flue gas temperature			(909)ᵇ	(902)ᵇ
		mean DDF rate (g/m²/h)			2691	1934
		no. of 6 h periods			16	9
		mean total deposit shedding rate (g/m²h)			1537	1329
		mean net deposit accumulation rate (g/m²/h)			1155	605
		mean net deposit accumulation rate (g/m²/h)ᶜ			957	
	<5000 g/m² (2447)ᵃ	mean flue gas temperature	(823)ᵇ	(823)ᵇ	(906)ᵇ	(874)ᵇ
		mean DDF rate (g/m²/h)	234	313	1245	577
		no. of 6 h periods	19	6	8	1
		mean total deposit shedding rate (g/m²/h)	185	124	793	356
		mean net deposit accumulation rate (g/m²/h)	49	189	452	221
		mean net deposit accumulation rate (g/m²/h)ᶜ	83		426	
<20 wt %	>5000 g/m²	mean DDF rate (g/m²/h)				
		no. of 6 h periods				
		mean total deposit shedding rate (g/m²/h)				
		mean net deposit accumulation rate (g/m²h)				
		mean net deposit accumulation rate (g/m²/h)ᶜ				
	<5000 g/m² (792)ᵃ	mean flue gas temperature	(773)ᵇ	(806)ᵇ		
		mean DDF rate (g/m²/h)	221	1913		
		no. of 6 h periods	17	1		
		mean total deposit shedding rate (g/m²/h)	147	660		
		mean net deposit accumulation rate (g/m²/h)	73	1253		
		mean net deposit accumulation rate (g/m²/h)ᶜ	139			

ᵃMean value of the deposit mass load. ᵇMean value of the flue gas temperature. ᶜMean value irrespective of probe surface temperature.

conditions (probe temperature = 500 °C, deposit mass < 5000 g/m², and a straw fuel share > 20 wt %) in Tables 4 and 5 but with different flue gas temperatures (below and above 850 °C), there is seen an increase in shedding frequency, and a small increase in shedding mass is also observed when the flue gas temperature is increased.

(d) Increased Fraction of Straw in the Fuel. Changes in fuel straw fraction in the fuel (from above to below 20 wt %) for the data sets with (probe temperature = 500 °C, deposit mass < 5000 g/², and flue gas temperature < 850 °C) show an increased shedding amount with decreased straw share. However, the mean shedding rate is low at lower straw fraction.

To summarize the main observations, the mean deposit shedding rate (shedding event amount times the shedding frequency) can be used as shown in Tables 4 and 5.

(1) The deposit shedding rates increased at high flue gas temperatures (>850 °C) and high probe deposit mass loads (>5000 g/m²), at which also high deposit formation rates are observed (DDF rate).

(2) The shedding rate is in most cases higher at a probe temperature of 500 °C than at a probe temperature of 600 °C. A possible reason could be partial melting and/or sintering of the innermost deposit layer (rich in K, Cl, and S)[24] at higher probe surface temperature. This could cause the adhesion strength of the deposit to increase at the higher probe surface temperatures.

(3) The deposit shedding process is a stochastic process, for which the amount of deposit shed varies, even at constant conditions (Figure 8). The deposit amount removed is probably strongly related to the strength of the innermost salt-rich deposit layer.
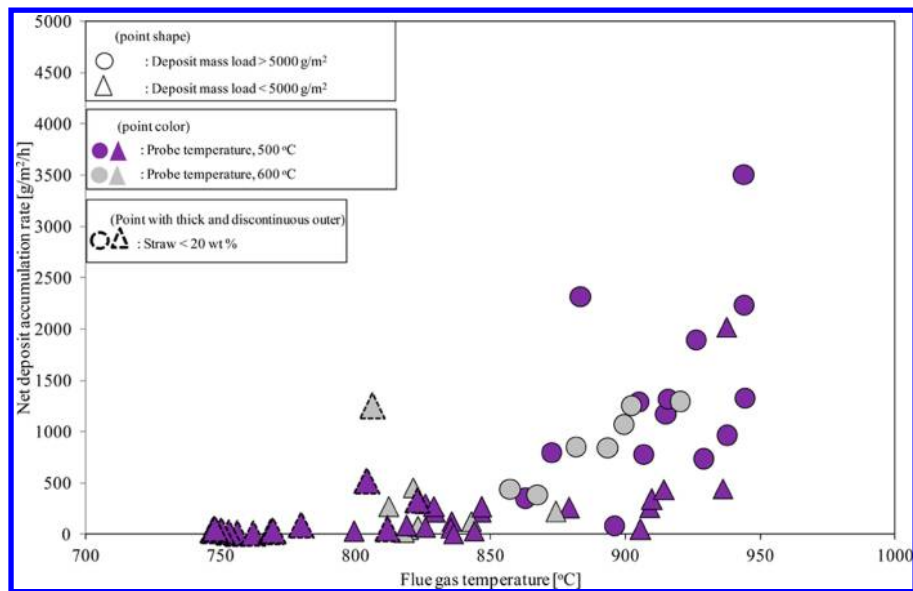
Net Deposit Accumulation Rate. The total deposit shedding rate was calculated by using eq 4:

total deposit shedding rate

$$= (\text{natural shedding rate} \times F)$$
$$+ (\text{sootblowing shedding rate} \times (1 - F)) \quad (4)$$

Here, F is the fraction of time of the 6 h interval when plant sootblowers were not in operation. The total deposit shedding rate as a function of the DDF rate is shown in Figure 9. It can be seen that with an increase in DDF rate, the total deposit shedding rate slightly increases. It is also evident that the total deposit shedding rate is lower than the DDF rate in most cases. This causes an accumulation of deposit mass on the probe with the passage of time. The accumulation of the deposits can be presented in the form of net deposit accumulation rate, a measure of the difference between the total shedding rate and the DDF rate. In addition, it is of interest for the plant operators to quantify deposit amount finally remaining on the superheater tubes as a common result of buildup and shedding. The net deposit accumulation rate was calculated by eq 5:

net deposit accumulation rate

$$= \text{DDF rate} - \text{total deposit shedding rate} \quad (5)$$

The calculated net deposit formation rate is shown in Table 6 for the changed conditions in flue gas temperature (above or below 850 °C), probe surface temperature (500 or 600 °C), straw fuel share (weight fraction of straw in the fuel above or below 20%), and deposit mass load (above or below 5000 g/m²). The main observations are the following.

Figure 10. Impact of flue gas temperature on the net deposit accumulation rate. Data points are from tests 1−5. The particular point shape represents the deposit mass load, and the color represents the probe surface temperature, whereas points (larger in size) with thick and discontinuous edges are representative of straw share in wood.

(1) The net deposit accumulation rate increases with increase in flue gas temperature (see Figure 10). Increased flue gas temperatures increase the fraction of molten ash as well as provide an increased content of gas phase alkali species, and both will lead to an increased deposit formation rate. The increase in DDF rate was larger than the increase in deposit shedding rate with increased flue gas temperature as shown in Table 6.

(2) The net deposit accumulation rate is low (452 $g/m^2/h$) at lower deposit mass load (<5000 g/m^2) on the probe, compared to a value of 1155 $g/m^2/h$ for deposit mass load > 5000 g/m^2 (Table 6, probe temperature = 500 °C, flue gas temperature about 900−910 °C, and straw share > 20 wt %).

(3) Generally, no clear tendency for the impact of probe surface temperature on net deposit accumulation rate was seen.

Deposit Removal by Using an Artificial Sootblowing Probe. The PIP needed in the sootblower jet to remove the probe deposits at different conditions was investigated using all three methods (1−3), and the results are summarized in Figure 11. It can be seen that increasing both probe surface temperatures and exposure times increased the PIP necessary to remove the deposits. It is also clear that deposits formed at a 500 °C probe temperature and with exposure time of <91 h could be removed with a PIP of <55 kPa. With an increase in probe surface temperature from 500 to 600 °C, the PIP needed to remove the deposits significantly increased. It is also interesting to note that the PIP seems to be independent of exposure time at the higher probe temperature. The higher probe surface temperature may cause partial melting and/or sintering of the innermost deposit layer (rich in K, Cl, and S).[24] This would enhance the adhesion between the deposit and superheater tube. At higher probe surface temperatures (>550 °C) and longer probe exposure times, a 2−10 mm thick layer formed on the downstream probe surface. The layer grew to make contact with the thick upstream layer. This ring-shaped layer will be more difficult to remove, because the ring must be broken by the sootblower. At lower surface temperatures (500 °C), the layer formed on the downstream side of the probe was
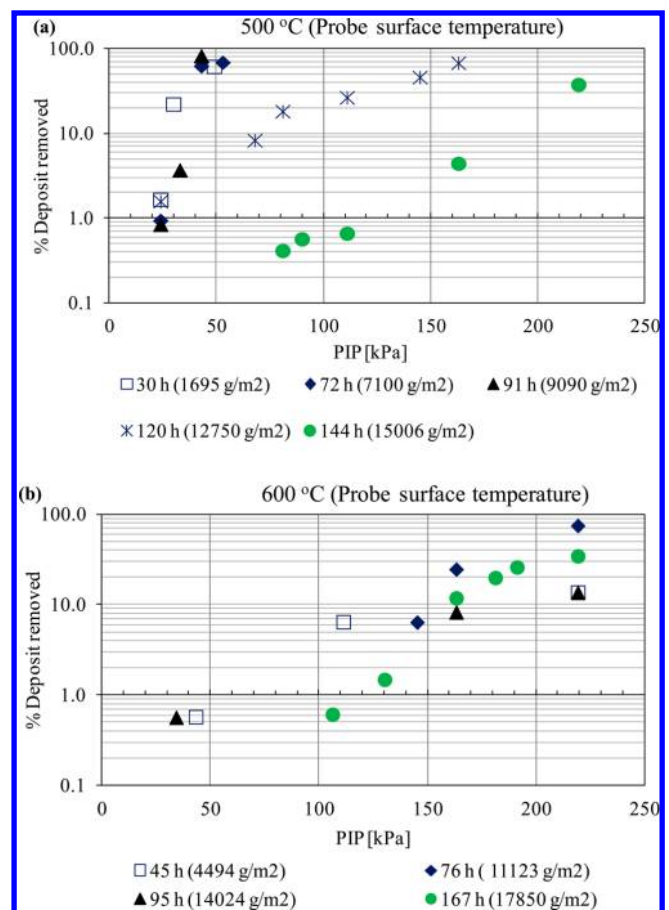
Figure 11. Percentage of deposits removed as a function of applied peak impact pressure (PIP) at different probe exposure times and deposit mass loads: (a) probe surface temperature = 500 °C; (b) probe surface temperature = 600 °C.

thin, and the distinct upstream layer was easy to remove using the artificial sootblower.
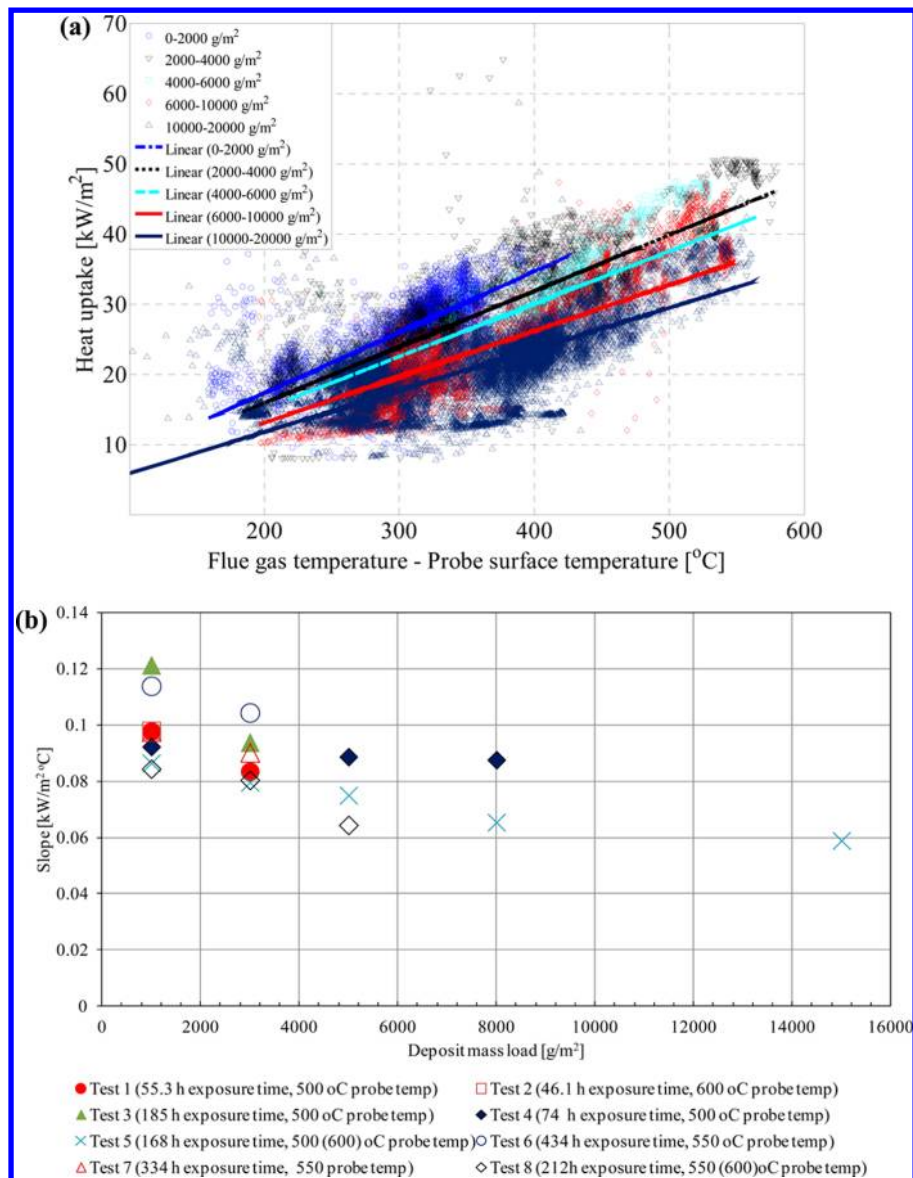
Figure 12. (a) Impact of temperature difference between flue gas and probe surface on heat uptake for different deposit mass loads for test 5. The slope is calculated by a linear fit using the equation $y = bx$. (b) Sensitivity of heat uptake with change in temperature difference between flue gas and probe surface for different deposit mass loads for all tests (1−8).

Probe Heat Uptake. The heat uptake in the probe, for different deposit mass loads during test 5, is shown Figure 12a as a function of the difference between flue gas temperature and probe surface temperature. It can be seen that when the deposit mass load is higher (>5000 g/m^2), the slope slightly decreases due to the insulation effect of the deposit layers. The slope for different deposit loads for each test was calculated, and the combined slopes for all tests for different probe mass loads are shown in Figure 12b. A moderate reduction in the probe heat uptake was observed with increase in mass load of deposits on the probe. All of the tests provided reasonably similar results. Additionally, it can be seen that up to a deposit mass load of 5000 g/m^2 the reduction in heat transfer is steeper, whereafter the steepness of the curve is reduced. This is consistent with the deposit layer being more pronounced on the upstream side, so that most of the heat uptake will occur through the downstream side.

CONCLUSIONS

The overall conclusions are the following:

(1) Video recordings revealed that deposit shedding was primarily through debonding, where a deposit layer is being removed due to a breakoff of the deposit from the tube surface.

(2) It was observed that the shedding process is a stochastic process, where the amounts of deposit shed are highly variable even at constant conditions. We believe the amount of deposit shed is strongly related to the strength of the innermost salt-rich deposit layer.

(3) The deposit shedding process was characterized by calculation of the average amount of deposit removed at a shedding event (g/m^2) and the frequency of the shedding events (h^{-1}) in 6 h periods. The average shedding event magnitude was 716 g/m^2 during natural deposit shedding and 805 g/m^2 during plant sootblowing-induced shedding events. The shedding frequencies were 0.81 and 0.89 h^{-1} during natural deposit shedding and plant sootblowing-induced

shedding events, respectively. On the basis of the shedding magnitude and frequency, it was possible to calculate a shedding rate ($g/m^2/h$).

(4) The deposit shedding rates increased at high flue gas temperatures (>850 °C) and high probe deposit mass loads (>5000 g/m^2) at which also high deposit formation rates are observed (DDF rate).

(5) The shedding rate is in most cases higher at a probe temperature of 500 °C than at a probe temperature of 600 °C.

(6) The net deposit accumulation rate increases with increase in flue gas temperature. Increased flue gas temperatures increase the fraction of molten ash as well as provide an increased content of gas phase alkali species, and both will lead to an increased deposit formation rate. The increase in DDF rate was larger than the increase in deposit-shedding rate with increased flue gas temperature.

(7) The net deposit accumulation rate is low (452 $g/m^2/h$) at lower deposit mass load (<5000 g/m^2) on the probe, compared to a value of 1155 $g/m^2/h$ for deposit mass load > 5000 g/m^2 (probe temperature = 500 °C, flue gas temperature about 900−910 °C, and straw share > 20 wt %).

(8) Generally, no clear tendency for the impact of probe surface temperature on net deposit accumulation rate was seen.

(9) A sootblower probe was used to investigate the needed PIP to remove the deposits. At lower temperatures (500 °C), the deposits formed at a exposure time of <91 h could be removed with a PIP of <55 kPa. At higher probe surface temperature (>550 °C), the PIP needed to remove the probe deposits significantly increases.

■ AUTHOR INFORMATION

Corresponding Author

*Phone: +45 45 25 28 49. Fax: +45 45 88 22 58. E-mail: paj@kt.dtu.dk.

Notes

The authors declare no competing financial interest.

■ ACKNOWLEDGMENTS

■ NOMENCLATURE

CCD = charge-coupled device

DDF rate = derivative-based deposit formation rate ($g/m^2/h$)

F = time fraction of 6 h period with no sootblower operation

$f_{nat,6}$ = mean natural deposit shedding frequency (h^{-1})

$f_{soot,6}$ = mean plant sootblowing deposit shedding frequency (h^{-1})

IDF rate = integrated deposit formation rate ($g/m^2/h$)

IFRF = International Flame Research Foundation

PIP = peak impact pressure (kPa)

■ REFERENCES

(1) Baxter, L. L. Ash deposition during biomass and coal combustion: a mechanistic approach. *Biomass Bioenergy* **1993**, *4*, 85−102.

(2) Nielsen, H. P. Deposition and high temperature corrosion in biomass-fired boilers. Ph.D. Thesis, Technical University of Denmark. 1998; ISBN 87-90142-47-0.

(3) Jenkins, B. M.; Baxter, L. L.; Miles, T. R., Jr.; Miles, T. R. Combustion properties of biomass. *Fuel Process. Technol.* **1998**, *54*, 17−46.

(4) Miles, T. R.; Miles, T. R., Jr.; Baxter, L. L.; Bryers, R. W.; Jenkins, B. M.; Oden, L. L. Boiler deposits from firing biomass fuels. *Biomass Bioenergy* **1996**, *10*, 125−138.

(5) Baxter, L. L. Influence of ash deposit chemistry and structure on physical and transport properties. *Fuel Process. Technol.* **1998**, *56*, 81−88.

(6) Sander, B.; Henriksen, N.; Larsen, O. H.; Skriver, A.; Ramsgaard-Nielsen, C.; Jensen, J. N.; Stærkind, K.; Livberg, H.; Thellefsen, M.; Dam-Johansen, K.; Frandsen, F. J.; van der Lans, R.; Hansen, J. Emissions, corrosion and alkali chemistry in straw-fired combined heat and power plants. *Proceedings of the 1st World Conference on Biomass for Energy and Industry*, Sevilla, Spain, June 5−9; James and James (Science Publishers): London, UK, 2009.

(7) Jensen, P. A.; Sander, B.; Dam-Johansen, K. Removal of K and Cl by leaching of straw char. *Biomass Bioenergy* **2001**, *20*, 447−457.

(8) Andersen, K. H.; Frandsen, F. J.; Hansen, P. F. B.; Wieck-Hansen, K.; Rasmussen, I.; Overgaard, P.; Dam-Johansen, K. Deposit formation in a 150 MWe utility PF-boiler during co-combustion of coal and straw. *Energy Fuels* **2000**, *14*, 765−780.

(9) Jensen, P. A.; Frandsen, F. J.; Hansen, J.; Dam-Johansen, K.; Henriksen, N.; Hörlyck, S. SEM investigation of superheater deposits from biomass-fired boilers. *Energy Fuels* **2004**, *18*, 378−384.

(10) Jensen, P. A.; Sørensen, L. H.; Hu, G.; Holm, J. K.; Frandsen, F.; Henriksen, U. B. Combustion experiments with biomass fuels and additives in a suspension fired entrained flow reactor − test of Ca and P rich additives used to minimize deposition and corrosion. *PSO Project: Biomass Dust Firing*; CHEC Report R0504, CHEC Research Centre, Technical University of Denmark: Lyngby, Denmark, 2005.

(11) Wu, H.; Glarborg, P.; Frandsen, F. J.; Dam-Johansen, K.; Jensen, P. A. Dust-firing of straw and additives: ash chemistry and deposition behavior. *Energy Fuels* **2011**, *25*, 2862−2873.

(12) Jensen, P. A.; Zhou, H.; Frandsen, F. J.; Hansen, J. Ash deposits removal in biomass power plant boilers. *Proceeding of 15th European Biomass Conference and Exhibition*, Berlin, Germany, May 7−11; ETA-Florence Renewable Energies: Florence, Italy, 2007.

(13) Tobiasen, L.; Skytte, R.; Pedersen, L. S.; Pedersen, S. T.; Lindberg, M. A. Deposit characteristics after injection of additives to a Danish straw-fired suspension boiler. *Fuel Process. Technol.* **2007**, *88*, 1108−1117.

(14) Frandsen, F. J. Ash formation, deposition and corrosion when utilizing straw for heat and power production. Doctoral Thesis, Technical University of Denmark, 2011; ISBN 978-87-92481-40-5.

(15) Jensen, P. A.; Stenholm, M.; Hald, P. Deposition investigation in straw-fired boilers. *Energy Fuels* **1997**, *11*, 1048−1055.

(16) Zbogar, A.; Frandsen, F.; Jensen, P. A.; Glarborg, P. Shedding of ash deposits. *Prog. Energy Combust. Sci.* **2009**, *35*, 31−56.

(17) Jameel, M. I.; Cormack, D. E.; Tran, H.; Moskal, T. E. Sootblowing optimization, Part 1: Fundamental hydrodynamics of a sootblower nozzle and jet. *Tappi J.* **1994**, *77*, 135−142.

(18) Ebrahimi-Sabet, S. A. A laboratory study of deposit removal by debonding and its application to fireside deposits in Kraft boilers. Ph.D. Thesis, Department of Chemical Engineering and Applied Chemistry, University of Toronto, 2001; ISBN 0-612-58923-4.

(19) Stitt, S. J.; Junker, H.; Baxter, L. L. Optimization of deposit removal in biofueled boilers: review of control systems, technologies and mechanisms, Report 02-1036. *Tech-wise* **2002**, 1−27.

(20) Zhou, H.; Frandsen, F. J.; Jensen, P. A.; Glarborg, P. PSO Project 4106, CHEC Report R0603, CHEC Research Centre, Technical University of Denmark, 2006.

(21) Zbogar, A.; Frandsen, F. J.; Jensen, P. A.; Hansen, J.; Glarborg, P. Experimental investigation of ash deposit shedding in a straw-fired boiler. *Energy Fuels* **2006**, *20*, 512−519.

(22) Pophali, A.; Emamia, B.; Bussmanna, M.; Tran, H. Studies on sootblower jet dynamics and ash deposit removal in industrial boilers. *Fuel Process. Technol.* **2011**, DOI: 10.1016/j.fuproc.2011.04.034.

(23) Kaliazine, A.; Cormack, D. E.; Ebrahimi-Sabet, A.; Tran, H. The mechanics of deposit removal in kraft recovery boilers. *J. Pulp Paper Sci.* **1999**, *25*, 418−424.

(24) Bashir, M. S.; Jensen, P. A.; Frandsen, F.; Wedel, S.; Dam-Johansen, K.; Wadenbäck, J.; Pedersen, S. T. Suspension-firing of biomass. Part 1: Full-scale measurements of ash deposit build-up. *Energy Fuels* **2012**, *26*, 2317−2330.

(25) Bashir, M. S.; Jensen, P. A.; Frandsen, F. J.; Wedel, S.; Dam-Johansen, K.; Pedersen, S. T.; Wadenbäck, J. Quantification of ash deposit build-up and removal in a straw and wood suspension-fired boiler. *Proceedings of 19th European Biomass Conference and Exhibition*, Berlin, Germany, June 6−10; ETA-Florence Renewable Energies: Florence, Italy, 2011.

(26) Nordgren, D.; Hedman, H.; Padban, N.; Boström, D.; Öhman, M. Ash transformations. *Fuel Process Technol.* **2011**, DOI: 10.1016/j.fuproc.2011.05.027.

(27) Frandsen, F. J. Utilizing biomass and waste for power production — a decade of contributing to the understanding, interpretation and analysis of deposits and corrosion products. *Fuel* **2005**, *84*, 1277−1294.

(28) Gjernes, E. Fuel flexibility at Amager unit 1 using pulverized fuels. *Proceedings of Power-Gen Europe*, Cologne, Germany, 2006.

(29) *IFRF Suction Pyrometer, User Information Document*; International Flame Research Foundation: Livorno, Italy, 2010.

(30) Bashir, M. S.; Jensen, P. A.; Frandsen, F.; Wedel, S.; Dam-Johansen, K.; Wadenbäck, J.; Pedersen, S. T. Ash transformation and deposit build-up during biomass suspension and grate firing: full-scale experimental studies. *Fuel Process. Technol.* **2012**, *97*, 93−106.